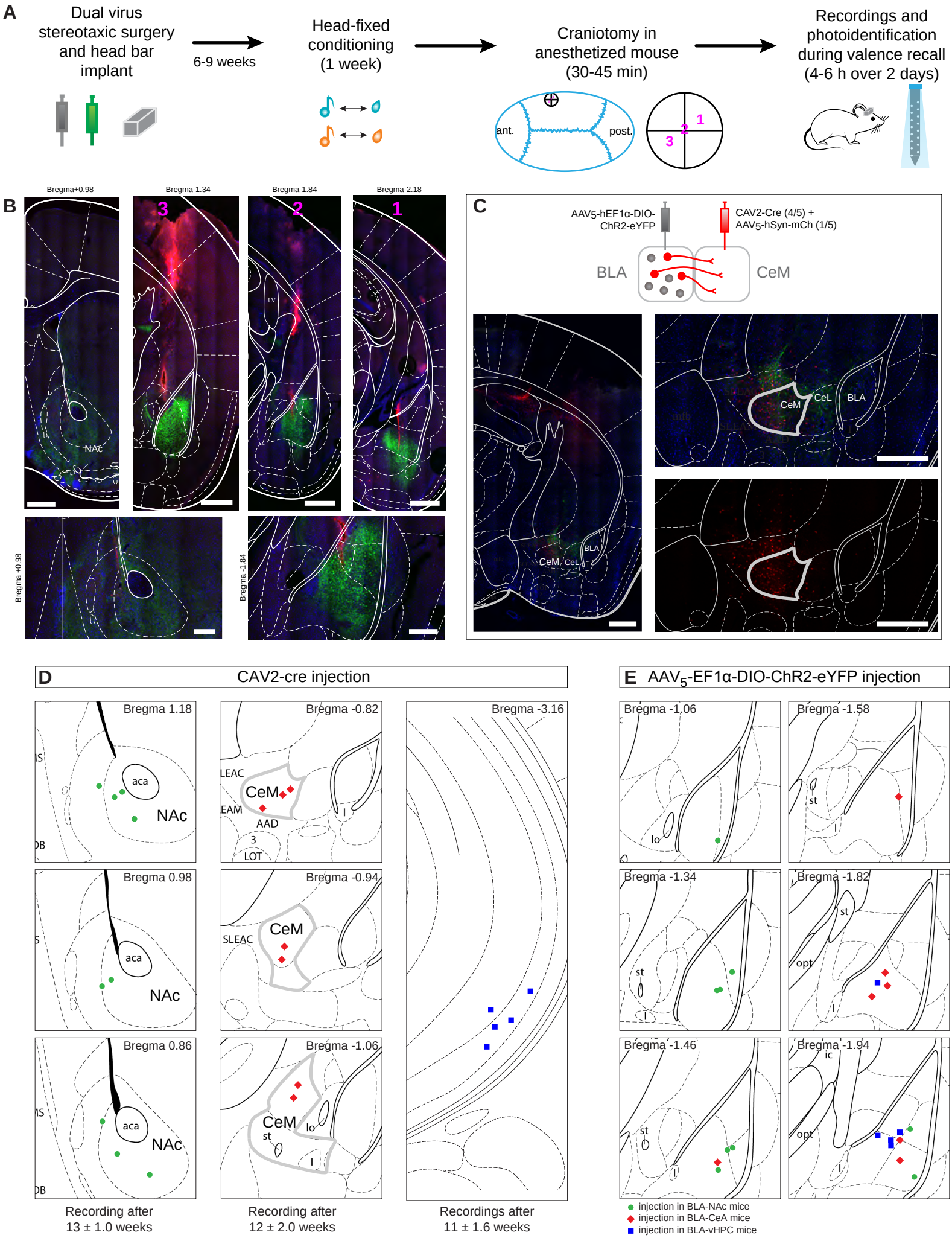
A
Dual virus stereotaxic surgery and head bar implant
6-9 weeks
Head-fixed conditioning (1 week)
Craniotomy in anesthetized mouse (30-45 min)
ant.
post.
Recordings and photoidentification during valence recall (4-6 h over 2 days)
B
Bregma+0.98
Bregma-1.34
Bregma-1.84
Bregma-2.18
NAc
LV
Bregma +0.98
Bregma -1.84
C
AAV5-hEF1α-DIO-ChR2-eYFP
CAV2-Cre (4/5) + AAV5-hSyn-mCh (1/5)
BLA
CeM
CeL
D
CAV2-cre injection
Bregma 1.18
Bregma -0.82
Bregma -3.16
Bregma 0.98
Bregma -0.94
Bregma 0.86
Bregma -1.06
aca
NAc
LEAC
CeM
EAM
AAD
LOT
SLEAC
Recording after 13 ± 1.0 weeks
Recording after 12 ± 2.0 weeks
Recordings after 11 ± 1.6 weeks
E
AAV5-EF1α-DIO-ChR2-eYFP injection
Bregma -1.06
Bregma -1.58
Bregma -1.34
Bregma -1.82
Bregma -1.46
Bregma -1.94
lo
st
opt
ic
injection in BLA-NAc mice
injection in BLA-CeA mice
injection in BLA-vHPC mice

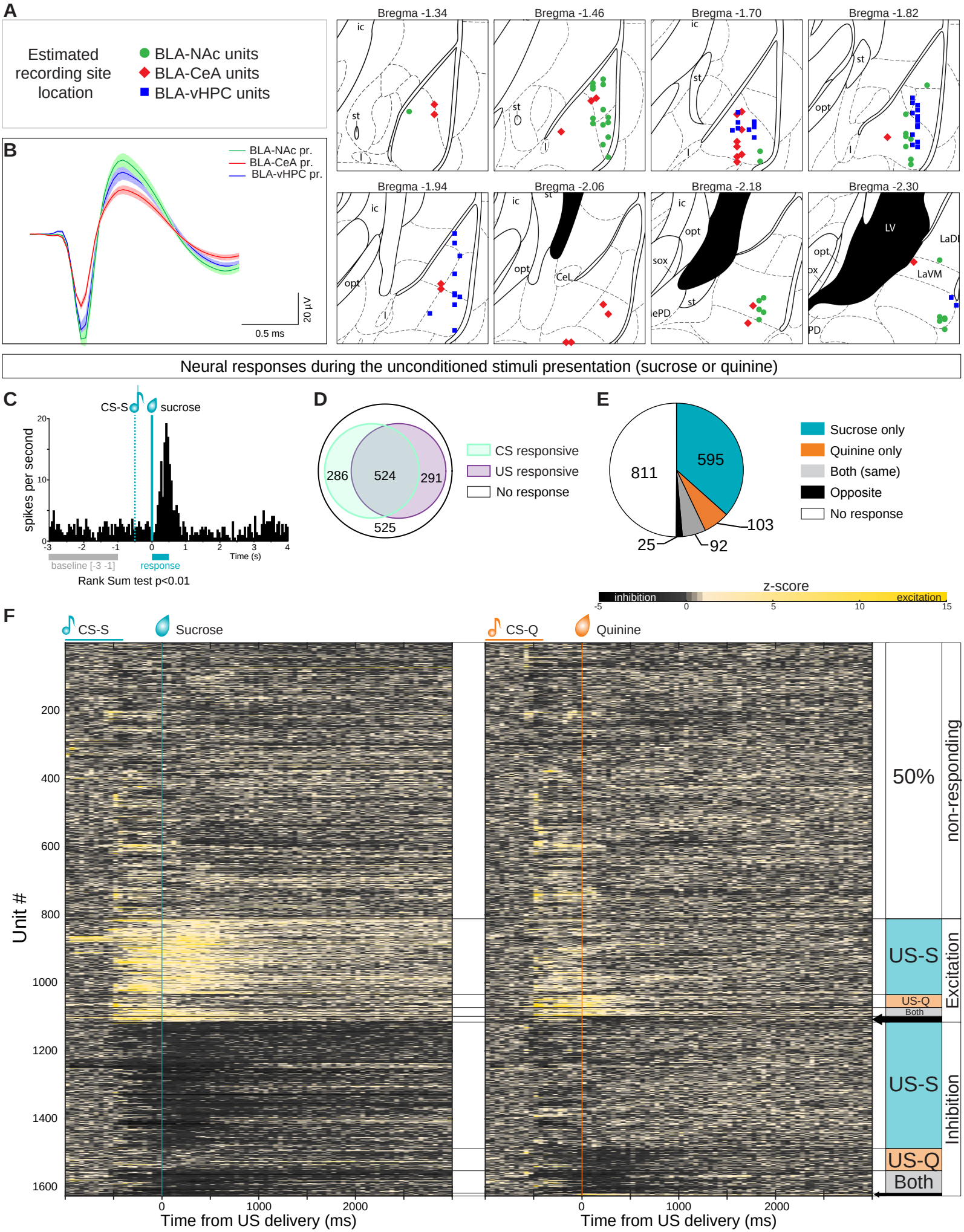
A
Estimated recording site location
BLA-NAc units
BLA-CeA units
BLA-vHPC units
Bregma -1.34
Bregma -1.46
Bregma -1.70
Bregma -1.82
Bregma -1.94
Bregma -2.06
Bregma -2.18
Bregma -2.30
ic
st
opt
sox
ePD
PD
LV
LaDl
LaVM
CeL
B
BLA-NAc pr.
BLA-CeA pr.
BLA-vHPC pr.
20 µV
0.5 ms
Neural responses during the unconditioned stimuli presentation (sucrose or quinine)
C
CS-S
sucrose
spikes per second
Time (s)
baseline [-3 -1]
response
Rank Sum test p<0.01
D
286
524
291
525
CS responsive
US responsive
No response
E
811
595
103
92
25
Sucrose only
Quinine only
Both (same)
Opposite
No response
z-score
inhibition
excitation
F
CS-S
Sucrose
CS-Q
Quinine
Unit #
Time from US delivery (ms)
50%
non-responding
US-S
US-Q
Both
Excitation
Inhibition

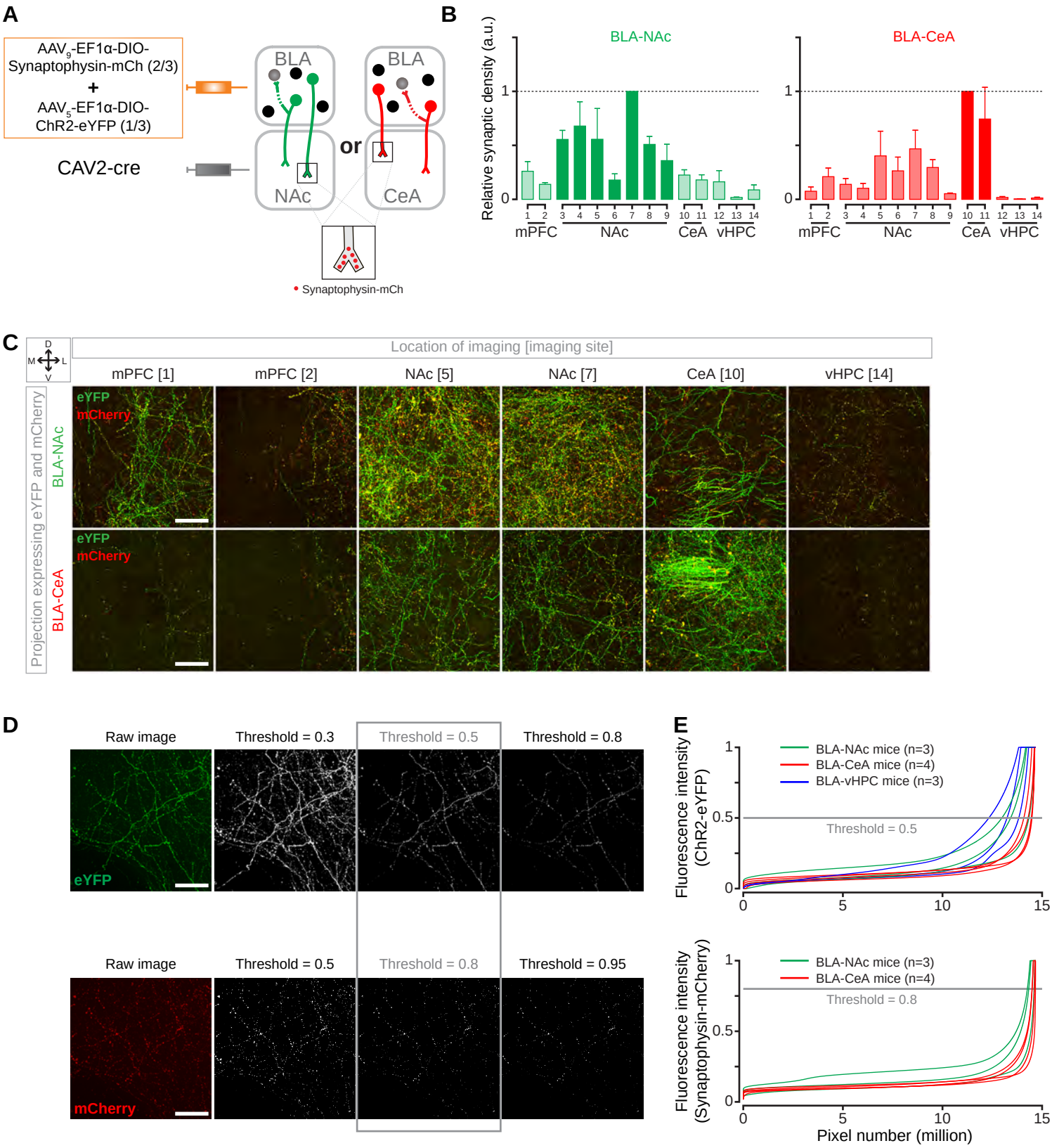
A
AAV9-EF1α-DIO-Synaptophysin-mCh (2/3)
+
AAV5-EF1α-DIO-ChR2-eYFP (1/3)
CAV2-cre
BLA
BLA
or
NAc
CeA
Synaptophysin-mCh
B
BLA-NAc
BLA-CeA
Relative synaptic density (a.u.)
mPFC
NAc
CeA
vHPC
C
Location of imaging [imaging site]
mPFC [1]
mPFC [2]
NAc [5]
NAc [7]
CeA [10]
vHPC [14]
Projection expressing eYFP and mCherry
BLA-NAc
BLA-CeA
eYFP
mCherry
D
Raw image
Threshold = 0.3
Threshold = 0.5
Threshold = 0.8
Threshold = 0.95
E
BLA-NAc mice (n=3)
BLA-CeA mice (n=4)
BLA-vHPC mice (n=3)
Fluorescence intensity (ChR2-eYFP)
Fluorescence intensity (Synaptophysin-mCherry)
Pixel number (million)

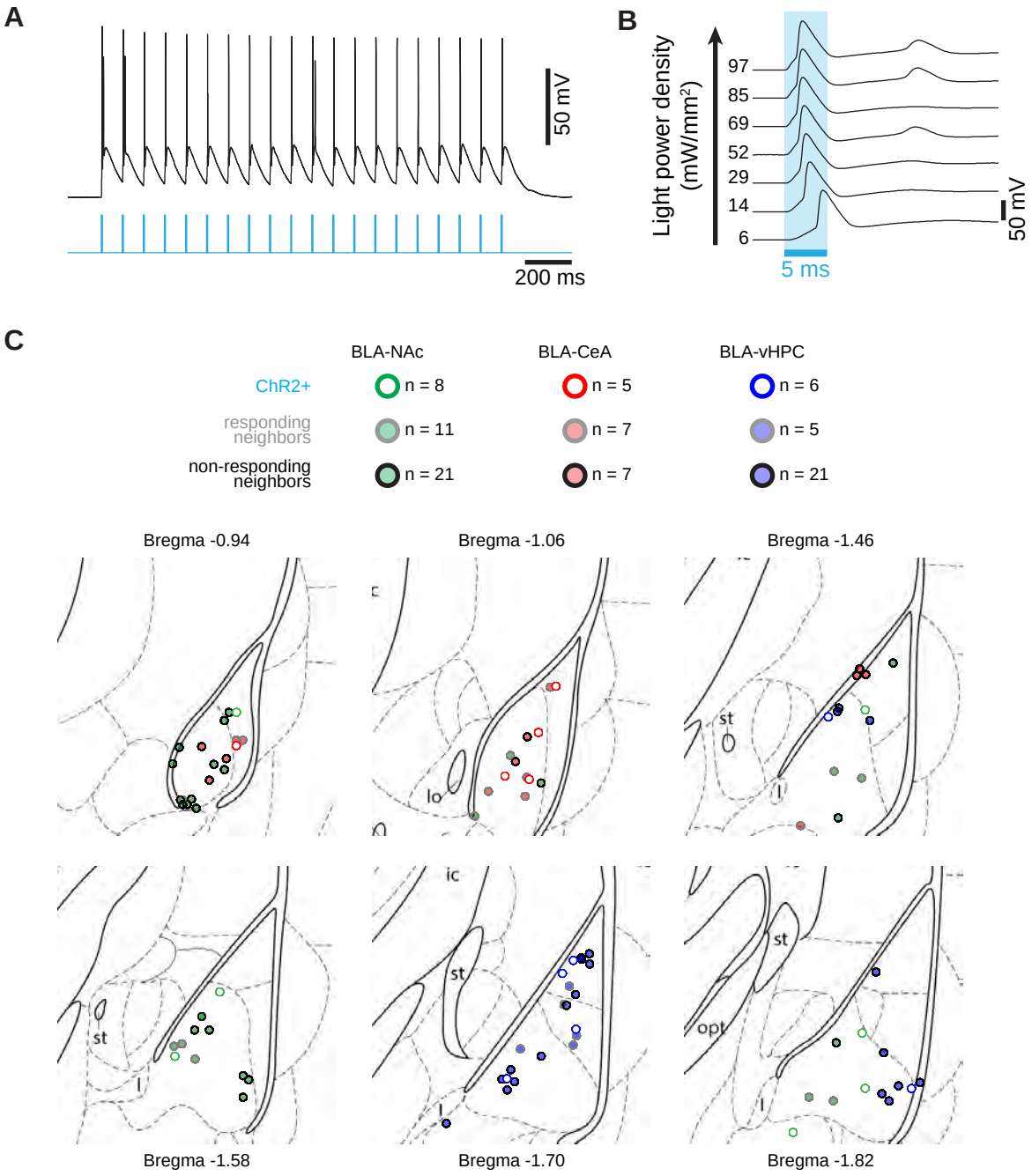
A
50 mV
200 ms
B
Light power density (mW/mm²)
97
85
69
52
29
14
6
50 mV
5 ms
C
BLA-NAc
BLA-CeA
BLA-vHPC
ChR2+
n = 8
n = 5
n = 6
responding neighbors
n = 11
n = 7
n = 5
non-responding neighbors
n = 21
n = 7
n = 21
Bregma -0.94
Bregma -1.06
Bregma -1.46
Bregma -1.58
Bregma -1.70
Bregma -1.82
st
lo
l
ic
opt

Neural responses during presentation of unconditioned stimuli (sucrose or quinine)

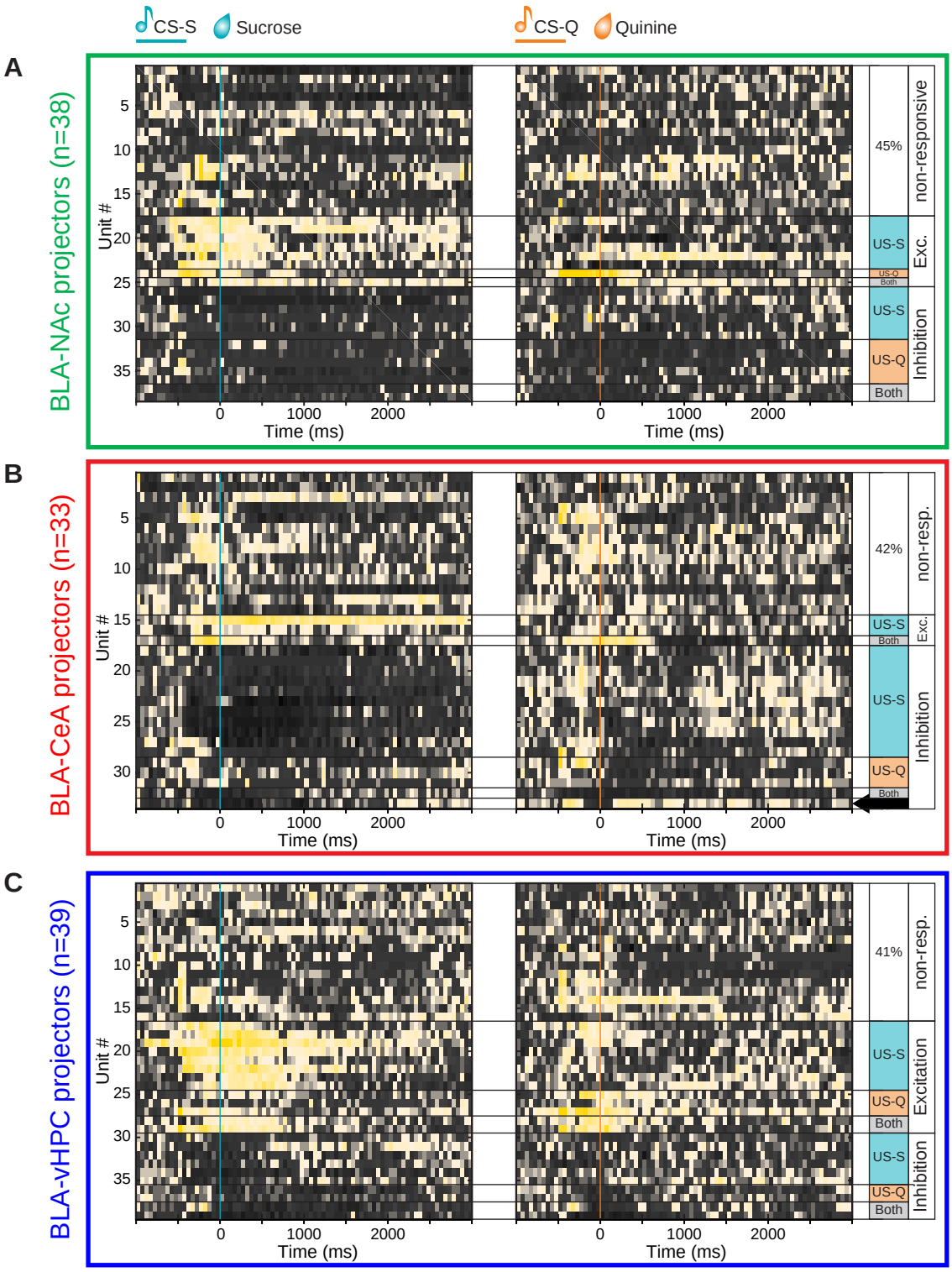

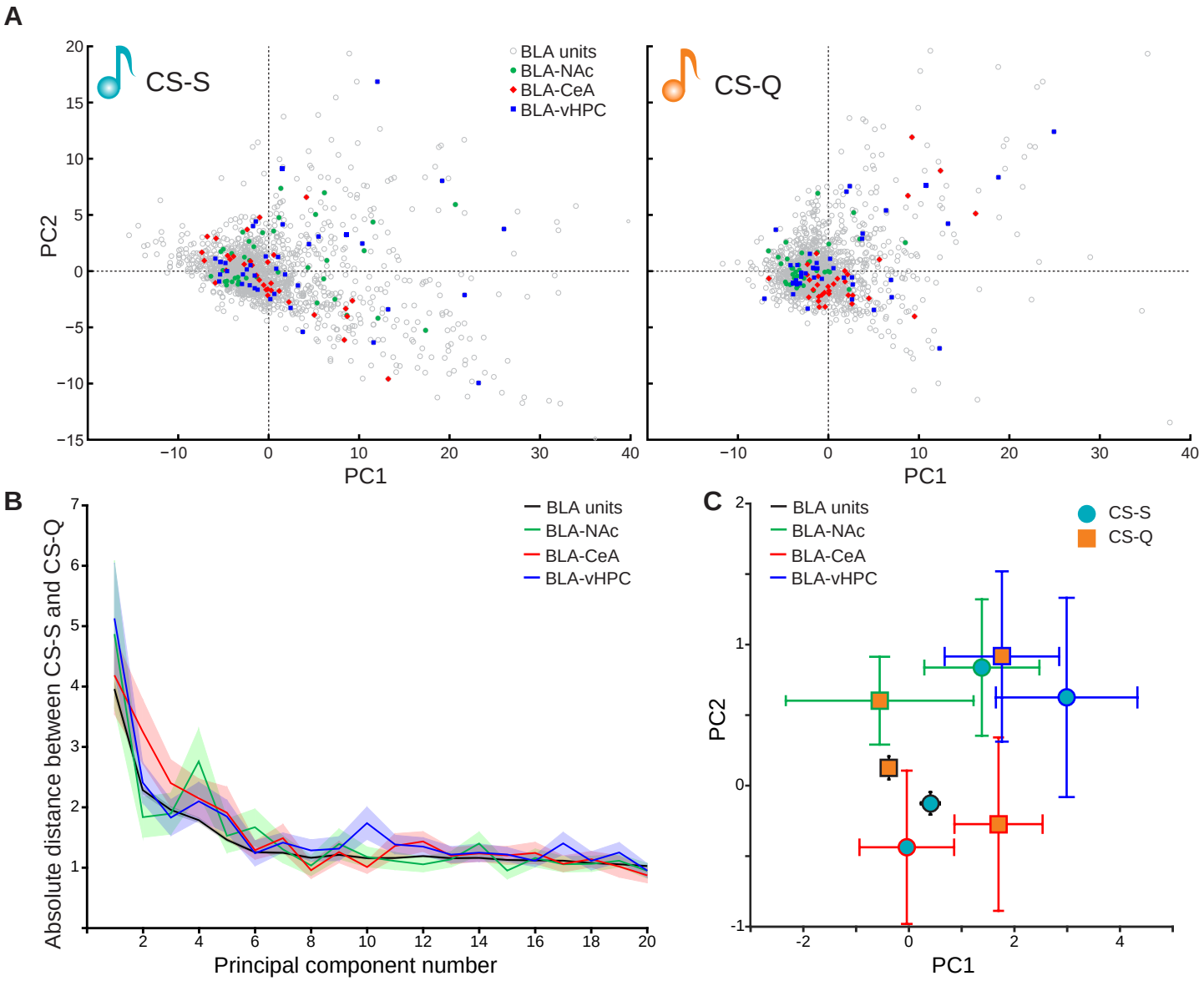
A
CS-S
CS-Q
BLA units
BLA-NAc
BLA-CeA
BLA-vHPC
PC1
PC2
B
Absolute distance between CS-S and CS-Q
Principal component number
C
CS-S
CS-Q
PC1
PC2

Neural responses during presentation of unconditioned stimuli (sucrose or quinine)

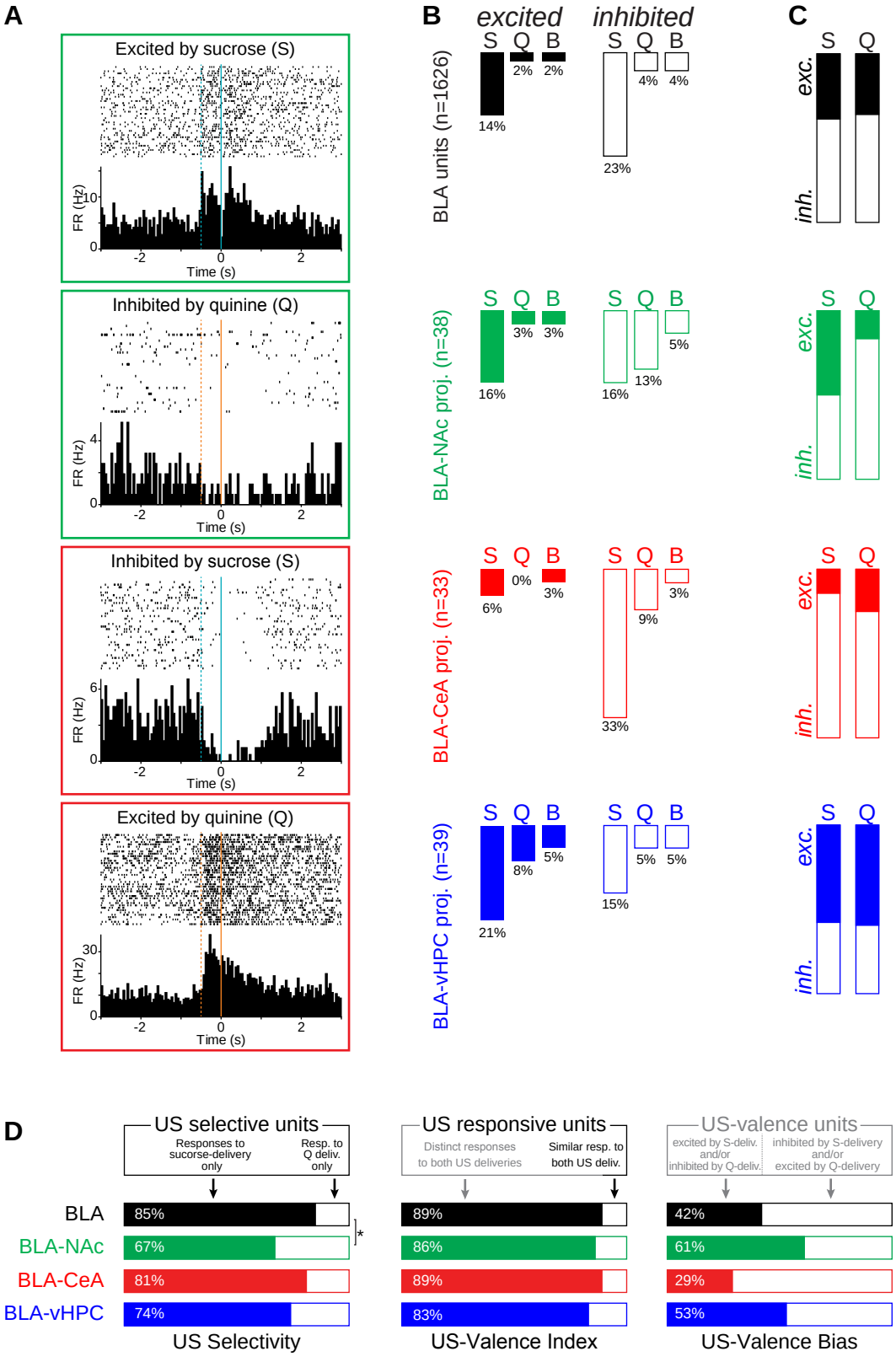

CS responses

Site of Cre Injection	Isolated units	CS-non responsive	CS-responsive	Excited by CS			Inhibited by CS			opposite to both CS		Projector number	Sound (kHz)	CS-US delay (ms)		Wilcoxon window (ms)	
				Sucrose	Quinine	Both	Sucrose	Quinine	Both	ExS-InQ	InS-ExQ		Sucrose	Sucrose	Quinine	Sucrose	Quinine
NAc	77	39	38	10	1	8	14	1	4	0	0	7	8	616	616	500	500
NAc	62	47	15	0	8	0	1	6	0	0	0	0	1	616	615	500	500
NAc	62	20	42	4	0	1	10	13	14	0	0	0	1	616	616	500	500
NAc	76	58	18	2	0	0	11	5	0	0	0	0	1	616	616	500	500
NAc	187	118	69	19	5	3	17	12	11	2	0	15	1	616	616	500	500
NAc	24	9	15	15	0	0	0	0	0	0	0	1	1	624	624	500	500
NAc	42	13	29	9	0	2	18	0	0	0	0	0	8	1004	1002	500	500
NAc	41	23	18	5	0	1	7	4	1	0	0	6	8	416	416	416	416
NAc	75	29	46	20	4	6	7	4	3	2	0	9	8	516	516	500	500
CeA	20	17	3	0	0	0	1	1	1	0	0	0	8	527	526	500	500
CeA	63	26	37	20	0	0	9	6	1	1	0	0	8	1018	1018	500	500
CeA	120	62	58	15	0	0	40	1	0	2	0	5	8	633	406	500	406
CeA	119	49	70	13	16	21	16	0	2	0	2	20	1	517	516	500	500
CeA	71	16	55	5	2	5	19	3	21	0	0	2	8	516	516	500	500
CeA	19	17	2	0	2	0	0	0	0	0	0	3	1	519	517	500	500
CeA	147	82	65	17	8	15	13	9	2	0	1	3	1	516	516	500	500
vHPC	109	45	64	21	7	14	12	3	7	0	0	15	1	526	433	500	433
vHPC	63	35	28	11	1	6	6	2	1	1	0	4	1	516	516	500	500
vHPC	80	43	37	8	6	2	7	3	10	0	1	2	1	516	516	500	500
vHPC	138	51	87	21	11	35	11	1	8	0	0	16	8	517	517	500	500
vHPC	31	17	14	13	0	0	1	0	0	0	0	2	8	517	517	500	500

CS responses

Experimental group	Isolated units	CS-non responsive	CS-responsive	Excited by CS			Inhibited by CS			opposite to both CS		Projector number	% 1kHz sound for sucorse	CS-US (ms)		Wilcoxon window (ms)	
				Sucrose	Quinine	Both	Sucrose	Quinine	Both	ExS-InQ	InS-ExQ			Sucrose	Quinine	Sucrose	Quinine
BLA	1626	816	810	228	71	119	220	74	86	8	4	110	52	594	579	496	488
BLA-NAc	38	15	23	10	0	3	3	2	5	0	0	38	56	626	626	491	491
BLA-CeA	33	16	17	4	5	3	4	0	1	0	0	33	43	607	574	500	487
BLA-vHPC	39	12	27	6	5	5	7	3	1	0	0	39	60	518	500	500	487

US responses

Experimental group	Isolated units	US-non responsive	US-responsive	Excited by US delivery			Inhibited by US delivery			opposite to both US	
				Sucrose	Quinine	Both	Sucrose	Quinine	Both	ExS-InQ	InS-ExQ
BLA	1626	811	815	223	38	26	372	65	66	17	8
BLA-NAc	38	17	21	6	1	1	6	5	2	0	0
BLA-CeA	33	14	19	2	0	1	11	3	1	0	1
BLA-vHPC	39	16	23	8	3	2	6	2	2	0	0

SUPPLEMENTAL FIGURE LEGENDS

Figure S1: Experimental design and histological confirmation of viral injections. Related to Figures 1, 2, 5, 6 and 7.

(A) After stereotaxic surgery and behavioral training, mice were briefly anesthetized prior to the recording session in order to open a small craniotomy above the BLA. After recovery, we recorded neural activity in the BLA using a 16 channel silicon optrode, while the animals were head fixed and discriminating between the cues of positive and negative valence.

(B) Confocal images of 50 µm coronal brain sections from the brain of a representative animal expressing ChR2 in BLA-NAc projectors. The first image corresponds to the CAV2-cre injection site in the NAc and the next three images correspond to the three recording tracks performed in this animal. The order of the track is indicated by the number at the top of each image. Each scale bar is 500 µm. Bottom images: enlarged image of the injection site of the CAV2-cre virus in the NAc (left) and enlarged image of the tip of the recording optrode in the BLA. Scale bars are 250 µm. Blue is DAPI, green represents eYFP and magenta corresponds to the red fluorescent microspheres left by the optrode during recording.

(C) To quantify the viral spread of the CAV2-cre virus within the CeA, we co-injected an anterograde virus expressing mCherry under the control of the synapsin promotor (100 nL of CAV2-cre + 25 nL of AAV_5-hSyn-mCh) in some of the recorded animals. A representative image of a slice showing DAPI in blue, eYFP in green, and mCherry in red (left), and enlarged images of the injection in the CeM are shown on the right, with only the mCherry channel displayed in the bottom right. Each scale bar is 500 µm.

(D) Center of the CAV2-cre viral injection in the NAc (green circles, n=9), CeM (red diamonds, n=7) or vHPC (blue squares, n=5) for all the animals analyzed after *in vivo* recordings.

(E) Center of viral injection of the cre-dependent AAV_5-EF1α-DIO-ChR2-eYFP virus in the BLA. The green circles correspond to the animals in the BLA-NAc experimental group, the red diamonds correspond to the animals in the BLA-CeA experimental group and the blue squares correspond to the animals in the BLA-vHPC experimental group.

Figure S2: Estimated position of silicone probe channels *in vivo,* and neural response of BLA units during the presentation of the unconditioned stimuli (US). Related to Figures 2, 5, 6 and 7.

(A) Estimated recording site location for phototagged units. Green circles represent the estimated location of BLA-NAc photoidentified units, red diamonds represent BLA-CeA photoidentified units and blue squares represent BLA-vHPC photoidentified units.

(B) Average action potential waveform of all the BLA-NAc projectors (green, n=38 units) all BLA-CeA projectors (red, n=33 units) and BLA-vHPC projectors (blue, n=39 units).

(C) Peristimulus time histogram (PSTH) of a single unit, representing the firing rate of the unit, relative to the sucrose delivery. For each unit, a Wilcoxon signed-rank test was used to determine if the neural response (firing rate) during the first 500 ms after the US delivery (blue bar, sucrose or quinine) is significantly different from the firing rate during a 2 s baseline window taken before the onset of the CS (gray bar, $^{**}p<0.01$).

(D) Of the 1626 units recorded from 21 mice, 32% responded to the CS and the US, while 18% of the neurons responded to the CS only, 18% to the US only, and 32% did not respond to the CS nor the US.

(E) Of the 1626 units, 50% had a significantly different firing rate during the first 500 ms after the unconditioned stimulus delivery compared to the 2 s baseline window. 37 % responded to the sucrose US only (US-S), 6% to the quinine US only (US-Q), 6% responded to both US in the same way and 1% responded to both unconditioned stimuli in an opposite manner (excited by one US, but inhibited by the other US).

(F) Heat maps representing the firing rate of all recorded units from 1 s before to 3 s after the outcome delivery. 19% of the units showed a significant excitatory response to one and/or the other US (yellow).

14% of the units showed excitation to the US-S while 4% were excited in response to the US-Q, and 2% were excited by both unconditioned stimuli. 32% of the units showed a significant inhibitory response to one and/or the other US. 23% were inhibited to the US-S, 4% showed an inhibitory response to the US-Q and 4% were inhibited by both unconditioned stimuli. The black arrows on the right of the heat maps point at the units responding to both unconditioned stimuli in an opposite manner (top arrow: excited by the US-S and inhibited by the US-Q (1%); bottom arrow: inhibited by the US-S and excited by the US-Q, (0.5%)).

Figure S3: Quantification of synaptic fluorescence from the axons of BLA projector populations. Related to Figure 3.

(A) A mix of two cre-dependent adeno-associated viral vectors were injected in the BLA containing 2/3 by volume of a serotype 9 vector under the control of a pan-neuronal promoter expressing Synaptophysin fused to a red fluorescent reporter (AAV_9-EF1α-DIO-Synaptophysin-mCherry) and 1/3 by volume of the serotype 5 vector under the control of a pan-neuronal promoter expressing channelrhodopsin-2 fused to an enhanced yellow fluorescent protein (AAV_5-EF1α-DIO-ChR2-eYFP). The retrograde canine adenovirus CAV2-cre was injected in the NAc or CeA.

(B) Quantification of the fraction of red fluorescent pixels (mCherry) per confocal image for each experimental group. The relative synaptic density represents the fraction of fluorescent pixels normalized within each animal to the reference location indicated in Figure 3B. The number of fluorescent pixels was obtained by thresholding the maximum intensity projection (MIP) of the confocal z-stack (>0.8). n=3 animals for each location in the BLA-NAc group, except mPFC (n=2), and n=4 for each location in the BLA-CeA group. Only one z-stack was obtained per animal per location.

(C) Representative MIPs of confocal images containing a section of (from left to right): the prelimbic (PL) or infralimbic (IL) prefrontal cortex (mPFC), the NAc medial core, the medial CeA and the posterior vHPC from one mouse expressing ChR2-eYFP in BLA-NAc projectors (top row), BLA-CeA projectors (bottom row). Scale bar 50 µm.

(D) Examples of fluorescence detection with different thresholds for ChR2-eYFP detection and Synaptophysin-mCherry detection. We chose 0.5 for ChR2-eYFP and 0.8 for Synaptophysin-mCherry. Thresholds were chosen by an observer blind to the experimental group of the animal, as well as the imaging location.

(E) Fluorescence intensity of every pixel across all images (14) from each animal, for green fluorescence (top panel, ChR2-eYFP) and red fluorescence (bottom panel, Synaptophysin-mCherry). The gray line represents the threshold for fluorescence detection.

Figure S4: Photoresponses of ChR2+ neurons and location of all patched cells. Related to Figure 4.

(A) Photoresponse of a ChR2+ neuron to a 10 Hz train (5 ms pulses) of blue light, recorded in current clamp.

(B) Evoked responses to light from a representative neuron expressing ChR2-eYFP, showing a decrease in firing latency as the light power density increases (6-97 mW/mm2).

(C) Location of all neurons recorded in whole-cell patch-clamp in the BLA. Each circle was reported from an image captured using differential interference contrast (DIC) microscopy. The color of the circle filling represents the experimental group from which the cell was recorded (no fill for ChR2+, colored fill for responding and non-responding neighbors). Among the ChR2+ group of cells, the color of the circle border represents the projection-target of the recorded cell, and among the responding and non-responding neighbor groups, the color of the fill represents the projection-target of the recorded cell: green, red and blue correspond to the ChR2-eYFP expressing cells in the BLA-NAc, BLA-CeA and BLA-vHPC groups respectively, the gray border corresponds to responding neighbors and the black border corresponds to non-responding neighbors.

Figure S5: Neural response of photoidentified BLA projectors to the consumption (sucrose) or presentation (quinine) of the unconditioned stimuli (US). Related to Figures 5, 6 and 7.
(A) Heat maps of neural activity from BLA-NAc photoidentified units in response to the sucrose outcome (teal, left) and to the quinine outcome (orange, right) displayed from 1 s before the delivery to 3 s after.
(B) Heat maps of neural activity from BLA-CeA photoidentified units in response to the sucrose outcome (teal, left) and to the quinine outcome (orange, right) displayed from 1 s before the delivery to 3 s after.
(C) Heat maps of neural activity from BLA-vHPC photoidentified units in response to the sucrose US (teal, left) and to the quinine US (orange, right) displayed from 1 s before the delivery to 3 s after.

Figure S6: Principal component analysis of cue-triggered neural dynamics for BLA neurons and BLA-NAc, BLA-CeA and BLA-vHPC projector populations. Related to Figure 6.
(A) CS-S (left) and CS-Q (right) triggered response for each neuron between -500 ms and 500 ms relative to the cue-onset, plotted along PC1 and PC2.
(B) The absolute distance between CS-S and CS-Q along each principal component, averaged across all neurons, and for each projector population.
(C) Standard errors of projected z-score time courses along the PC1 and PC2 across neurons in each populations for the rewarding (CS-S) and aversive cues (CS-Q).

Figure S7: Classification of the different neuronal responses to the delivery of the unconditioned stimuli (US). Related to Figure 7.
(A) Perievent raster histograms of two units photoidentified as NAc projectors (two top panels) and two units photoidentified as CeA projectors (two bottom panels). For the BLA-NAc projectors, the first is showing an excitatory response after the sucrose delivery, and the second is showing an inhibitory response after the quinine delivery. For the BLA-CeA, the first unit is inhibited by the sucrose delivery while the second is excited by the quinine delivery.
(B) Distribution of units excited or inhibited by the delivery of the US-S (S), US-Q (Q) and both unconditioned stimuli (B) in all the BLA units (black), in the BLA-NAc photoidentified units (green), in the BLA-CeA photoidentified units (red) and in the BLA-vHPC photoidentified units (blue).
(C) Proportion of units excited and inhibited by the sucrose delivery (S) or the quinine delivery (Q) in the four neural populations.
(D) Characterizing the representation of the sucrose and quinine US in the BLA, and in each of the three projector populations. US selectivity (left panel): proportion of US responsive cells responding exclusively to the sucrose versus to the quinine delivery. US-Valence index (middle panel): proportion of US responsive units showing distinct responses to the unconditioned stimuli (either selective or opposite responses to sucrose and quinine deliveries), among all the US responsive units. US-Valence bias (right panel): US-Valence bias is the ratio of the number of neurons excited by a sucrose delivery and/or inhibited by a quinine delivery to the number of US responsive units showing distinct responses to sucrose and quinine. Gray lettering indicates the relationship between the middle and right panels – units under gray lettering in the middle panel are sufficient to compute the US-Valence bias metric.

Movie S1: Positive and negative valence retrieval. Related to Figure 1.
Behavior of a representative mouse during the recall of the positive valence association (1 kHz tone followed by sucrose delivery) and for the negative valence association (8 kHz tone followed by quinine delivery). The licking behavior (infra-red beam-breaks), the event triggers and the sound wave were recorded during every training session and during the electrophysiological recordings. The frequency of the tones associated with the rewarding and aversive outcomes were counterbalanced between animals (see Table S1).

Table S1: Number of units in every response type to the CS or the US delivery, and experimental parameters for each animal and in experimental groups. Related to Figure 7.

Both: neurons responding to both cues (CS-S and CS-Q) or to both deliveries (sucrose and quinine) in the same qualitative way.

Opposite to both CS: units responding to both cues in an opposite way. ExS-InQ, excited by CS-S and inhibited by CS-Q; InS-ExQ, inhibited by CS-S and excited by CS-Q.

Opposite to both US: units responding to both deliveries in an opposite way. ExS-InQ, excited by the sucrose delivery and inhibited by the quinine delivery; InS-ExQ, inhibited by the sucrose delivery and excited by the quinine delivery.

SUPPLEMENTAL EXPERIMENTAL PROCEDURES

Animals and Stereotaxic Surgery.

Adult wild-type male C57BL/6 mice (39 mice), aged 8-10 weeks (Jackson Laboratory, Bar Harbor, ME) were used for experiments. Following surgery, animals were maintained with a reverse 12 hours light/dark cycle with *ad libitum* food and water for ~11 weeks to allow viral expression. All procedures for handling animals were in accordance with the guidelines from NIH and with approval from the MIT Committee on Animal Care (CAC). All surgeries were conducted under aseptic conditions using a digital small animal stereotaxic instrument (David Kopf Instruments, Tujunga, CA).

Mice were anaesthetized with isoflurane (5 % for induction, 1.5-2.0 % after) in the stereotaxic frame for the entire surgery and their body temperatures were maintained with a heating pad. In order to express ChR2-eYFP only in basolateral amygdala (BLA) neurons projecting to a specific downstream target, an adeno-associated virus serotype 5 (AAV_5) carrying channelrhodopsin-2 (ChR2) fused to an enhanced yellow fluorescent protein (eYFP) in a double-floxed inverted open reading frame (DIO) under the control of elongation factor-1α promoter (~500 nL of AAV_5-EF1α-DIO-ChR2-eYFP) was injected into the BLA at stereotaxic coordinates from bregma: -1.60 mm AP, +3.32 mm ML and -4.90 mm DV. Concurrently, canine adenovirus-2 (CAV2) carrying cre-recombinase (or a 1:1 mixture of CAV2-cre and herpes simplex virus (HSV) carrying a cre-recombinase fused to mCherry and under an EF1α promoter; HSV-hEF1α-mCherry-IRES-cre) was injected into the nucleus accumbens (NAc), the medial part of the central amygdala (CeA) or the ventral hippocampus (vHPC) using the following coordinates from bregma: NAc: 1.30 mm AP, +0.80 mm ML and -4.70 mm DV; CeM: -0.80 mm AP, +2.35 mm ML and -5.20 mm DV; vHPC: -3.55 mm AP, +3.50 mm ML and -4.00 mm DV.

For two BLA-CeA surgeries, CAV2-cre was mixed with an AAV_5-hSyn-mCherry (4:1) in order to quantify the spread of the virus in the downstream target. Most of the mCherry expression was in the medial part of the central amygdala (CeM), but some cells in the lateral part of the central amygdala (CeL) expressed mCherry indicating that CAV2-cre could have transduced terminals in the CeL. To be conservative, neurons expressing ChR2-eYFP in the BLA after CAV2-cre injection in the CeM, were classified as CeA projectors (Figure S1C).

For the quantification of synaptic contacts of the BLA-NAc and BLA-CeA projectors, we injected a 1:2 mix of the cre-dependent vector expressing ChR2-eYFP (AAV_5-EF1α-DIO-ChR2-eYFP) and an adeno-associated virus serotype 9 (AAV_9) carrying synaptophysin fused to the red fluorescent protein mCherry in a double-floxed inverted open reading frame (DIO) under the control of elongation factor-1α promoter (AAV_9-EF1α-DIO-Synaptophysin-mCherry, Figure S3).

AAV_5 virus aliquots were obtained from the University of North Carolina Vector Core (Chapel Hill, NC). HSV and AAV_9 vectors were packaged by the Massachusetts Institute of Technology viral vector core facility (Cambridge, MA, USA) and the CAV2 vector was obtained from the Kremer lab (CNRS, Montpellier, France).

Injections were conducted with a beveled 33 gauge microinjection needle facing the posterior side for the BLA, the NAc and the vHPC injections and facing the midline for the CeM injection. 10 µL microsyringes (nanofil; WPI, Sarasota, FL) were used to deliver viral suspensions at a rate of 100 nL/min using a microsyringe pump (UMP3; WPI, Sarasota, FL) and its controller (Micro4; WPI, Sarasota, FL). After completing the injection, the needle was raised 100 µm for an additional 10 minutes to allow the virus to diffuse at the injection site and then slowly withdrawn.

Immediately after retracting the injection needle, a small aluminum head-bar (2 cm*2 mm*2 mm) was placed on the skull 1.5 mm anterior to the bregma along with one reference and one ground pin contacting the dura mater 0.5 mm anterior to the left lambdoid suture. The skull above the BLA was covered with soft paraffin to prevent obstruction of this area. The three elements (head bar, ground pin and reference pin) were cemented using one layer of adhesive cement (C&B metabond; Parkell,

Edgewood, NY) followed by a layer of cranioplastic cement (Dental cement; Stoelting, Wood Dale, IL). After the cement dried, the craniotomy was covered with a silicone gel (Kwik-Sil Adhesive, WPI, Sarasota, FL) to protect the craniotomy until the bone sealed naturally.
After surgery, the animal's body temperature was maintained using an infra-red heat lamp until it fully recovered from anesthesia. Behavioral training was started about 11 weeks after viral surgery and *in vivo* electrophysiological recordings were conducted approximately 12 weeks following surgery.

Pavlovian valence conditioning

Behavioral conditioning. About 11 weeks after surgery, mice were conditioned in a modified head-fixed stereotaxic apparatus. One day prior to starting the conditioning protocol, the mice were food restricted and pre-exposed to 30% sucrose. On the first day of conditioning, mice were habituated to the conditioning apparatus by allowing them to explore the apparatus freely for 15 minutes. They were then head-fixed in front of a servo motor (Adafruit Industries, New York, NY) holding two small tubes separated by an angle of 16 degrees (Movie S1). Two speakers wired to a mini sound amplifier (Pyle Audio) were placed on either side of the mouse. Small drops (3 µL) of sucrose and quinine were delivered through the two small tubes (one tube per solution) via two solenoid valves (Parker, Cleveland, OH). In order to monitor the behavior of the mouse, the licking behavior was measured through an infra-red beam break controlled by an Arduino board (SmartProjects, Italy).
The sound amplifier, solenoid valves and servomotor were triggered with a custom software written in Labview (National instruments, Austin, TX) powered by NIDAQ-6251 and Arduino hardware. Throughout every training session (1 h), the sound wave, the electronic trigger for the amplifier and the solenoid valves, and the beam breaks were recorded with a Digidata 1440 board and pClamp9 software (Molecular Devices, Sunnyvale, CA).
In the behavioral task, two auditory cues were delivered in anticipation of either sucrose or quinine delivery (1 and 8 kHz, counterbalanced between animals: 1 kHz predicted sucrose for 11/21 animals, see Table 1). In the BLA and in the BLA projector populations, we found that populations had slightly higher percentages of units responding to 8 than to 1 kHz: 22% versus 15% in the BLA; 29% versus 11% in BLA-NAc projector population; 21% versus 18% in BLA-CeA projector populations; 28% to 26% in BLA-vHPC projector population). Over the first 2 days of training, one auditory cue was played every 22±8 s (inter-trial interval (ITI) randomly chosen between 16, 20, 24, and 28 s). 200 ms after cue onset, the servo motor positioned one of the tubes in front of the mouth of the animal allowing the mouse to lick the drop of 30 % sucrose solution which was delivered 500 ms after cue onset. After mice acquired this first association, indicated by exhibiting anticipatory licking (prior to the movement of the servo motor and the sucrose delivery), we introduced a second auditory cue paired with a delivery of 1 mM quinine solution in the other tube (Figure 1, Movie S1). On the first day of exposure to quinine, only 10-20% of the trials were of negative valence (quinine deliveries). This proportion of quinine trials was incrementally increased each day until reaching 50%. After about 6 days of training, the mice learned both associations, and we recorded neural activity in the BLA. During the electrophysiological recordings, the behavior of the mouse was recorded with a digital webcam.

Learning criteria. At the end of each training session, the performance of the animals was quantified using custom software in MATLAB written by PN. The animals were classified as knowing both associations when their performance for the positive association (PA=sucrose trials with licks / number of sucrose trials) and their performance for the negative association (NA=quinine trials without licks / number of quinine trials) were both above 70%. Upon reaching criteria, recordings were obtained from the animal's BLA, and the data was used only if the animal's PA and NA performance were each above 60% during the recording session and if there were at least 20 successful sucrose and 20 successful quinine trials within that session.

Ex vivo electrophysiology

Brain tissue preparation. About ten weeks after dual viral injections in the BLA and NAc, CeA, or vHPC, 11 mice were anesthetized with 90 mg/kg pentobarbital and perfused transcardially, after clamping the abdominal aorta, with 10 mL of artificial cerebrospinal fluid (ACSF, at ~4°C) containing (in mM): 75 sucrose, 87 NaCl, 2.5 KCl, 1.3 NaH_2PO_4, 7 $MgCl_2$, 0.5 $CaCl_2$, 25 $NaHCO_3$ and 5 ascorbic acid. The brain was then extracted and glued (Roti coll 1; Carh Roth GmbH, Karlsruhe, Germany) to the platform of a semiautomatic vibrating blade microtome (VT1200; Leica, Buffalo Grove, IL). The platform was then placed in the slicing chamber containing modified ACSF at 4°C. Coronal sections of 300 µm containing the NAc, CeA, vHPC and/or BLA were collected in a holding chamber filled with ACSF saturated with 95% O_2 and 5% CO_2, containing (in mM): 126 NaCl, 2.5 KCl, 1.25 NaH_2PO_4, 1.0 $MgCl_2$, 2.4 $CaCl_2$, 26.0 $NaHCO_3$, and 10 glucose. Recordings were started 1 h after slicing, and the temperature was maintained at approximately 31°C both in the holding chamber and during the recordings.

All viral injection sites were checked and imaged with a camera (Hamatsu Photonics K.K., Japan) attached to the microscope (BX51; Olympus, Center Valley, PA). The slice images were registered to the mouse brain atlas (Paxinos and Watson) and the center of the injection was considered the brightest point of the fluorescence. If the injection site was outside the NAc, the CeA or the vHPC, data was not collected from that animal.

Whole-cell patch-clamp recording. Recordings were made from visually identified neurons expressing ChR2-eYFP and non-expressing neighboring cells. Patched cells were filled with Alexa Fluor (AF) 350 and biocytin. Voltage and current-clamp recordings of BLA projectors were conducted using glass microelectrodes (4-7 MΩ) shaped with a horizontal puller (P-1000, Sutter, CA) and filled with a solution containing (in mM): 125 potassium gluconate, 20 HEPES, 10 NaCl, 3 MgATP, 8 biocytin and 2 Alexa Fluor 350 (pH 7.25-7.4; 280-290 milliOsmol). Recorded signals were amplified using a Multiclamp 700B amplifier (Molecular Devices, Sunnyvale, CA). Analog signals were digitized at 10 kHz using a Digidata 1440 and recorded using the pClamp10 software (Molecular Devices, Sunnyvale, CA). Oxygenated ACSF was perfused onto the slice via a peristaltic pump (Minipuls3; Gilson, Middleton, WI) at ~3 mL/min. Cells were confirmed to express ChR2 based on a constant inward current response to a 1 s constant blue light pulse in voltage clamp.

Data analysis. Off-line analysis was performed using Clampfit software (Molecular Devices, Sunnyvale, CA). Light evoked latencies of action potentials (AP) and excitatory postsynaptic potentials (EPSP) were measured for each cell for 20 pulses of a 2 second train at 10 Hz with 5 ms pulses (Figure S4A). Latencies were measured from the onset of the light pulse to the peak of the AP or EPSP.

Histology. The location of all recorded neurons was checked after the recording (Figure S4). Co-localization of AF 350 and ChR2-eYFP was confirmed with confocal microscopy for the cells that were recovered with biocytin-streptavidin staining. For each experiment, the slices containing a retrograde viral injection (NAc, CeA or vHPC) or a recorded neuron (BLA) were fixed overnight at 4°C in 4 % PFA, and then kept in PBS. Slices containing patched neurons were incubated for 2 hours in streptavidin-CF405 (2 mg/ml, dilution 1:500, Biotium, Hayward, CA), mounted on microscope slides with PVA-DABCO and imaged under the confocal microscope (Figure 4).

***In vivo* electrophysiology**

Pre-recording craniotomy. At 11±1 weeks after surgery, and after learning the two associations for one week, mice were briefly anesthetized with isoflurane (5% for induction, 1.5% after) while their body temperature was controlled with a heating pad, in order to open a small craniotomy over the BLA. The stereotaxic coordinates were re-measured for every animal from the center of the head-bar (cemented 1.5 mm anterior to bregma). When the craniotomy was open, with the dura removed, and the blood cleaned away, it was covered with soft paraffin, and the mice were placed in a new recovery cage while their body temperature was maintained using a heat lamp until they fully recovered from anesthesia.

In Vivo Electrophysiological Recordings and Phototagging with ChR2. Once the mice recovered from the craniotomy surgery (at least 30 min), they were head-fixed and a silicon optrode (A1x16-Poly2-5mm-50s-177, Neuronexus, Ann Arbor, MI) coated with red fluorescent latex microspheres (Lumafluor Inc.) was inserted at the strereotaxic coordinates of the posteriorlateral BLA and lowered from the surface of the cortex for 3 mm at 10 µm/s using a motorized actuator (Z825B - 25 mm Motorized Actuator, Thorlabs, Newton, NJ, USA) mounted on a shuttle (460A linear stage, Newport, Irvine CA, USA) fixed to the stereotaxic arm. During the insertion of the electrode, auditory cues associated with sucrose and quinine deliveries were presented every 42±8 s. Then the optrode was lowered at 1-2 µm/s, and we applied 200 ms blue laser pulses (15 mW, Extended Figure 4A) every 50 µm, to search for light evoked responses.

When we observed a neural response to the light, we waited for 5 min to let the tissue stabilize around the recording probe. We then started a recording session using a RZ5D TDT system (Tucker-Davis Technologies, Alachua, FL, USA) while presenting at least 30 sucrose and 30 quinine trials randomly intermixed. Following completion of the task, a photoidentification session using a 473 nm laser was conducted, during which pseudorandomly dispersed stimulations of 1 s constant light, 10 s of 1 Hz (5 or 10 ms pulses), 2 s of 10 Hz (5 ms pulses) and 100 ms of 100 Hz (5 ms pulses) were delivered, with at least 5 iterations of each. We then stopped the recording and started moving the optrode again at 1-2 µm/s. The electrode was lowered at least 200 µm before starting a new recording session. When we reached the bottom of the BLA (-4.2 mm from brain surface) we pulled the electrode up at 5 µm/s (until -3mm from brain surface) and then at 10-15 µm/s. The electrode was then inserted again about 150 µm anterior and 150 µm medial to the first recording site. At the end of the second track the craniotomy was sealed with silicone gel (Kwik-Sil Adhesive, WPI, Sarasota, FL) in order to protect the brain until the next day of recording. During the second day of recording, the same procedure was repeated and the animals were then sacrificed in order to verify the viral expression and the location of the recording electrode.

Histology. After the second day of recording, the mice were anesthetized with pentobarbital sodium and transcardially perfused with ice-cold ringer's solution followed by ice-cold 4% paraformaldehyde (PFA) in PBS (pH 7.3). Extracted brains were fixed in 4% PFA overnight and then equilibrated in 30% sucrose in PBS. 40 µm thick coronal sections were sliced using a sliding microtome (HM430; Thermo Fisher Scientific, Waltham, MA) and stored in PBS at 4°C until processing for histology. Sections were then incubated with a DNA specific fluorescent probe (DAPI: 4',6-Diamidino-2-Phenylindole (1:50,000)) for 30 minutes and lastly washed with PBS-1X followed by mounting on microscope slides with PVA-DABCO.

Analysis of in Vivo Awake-Behaving Electrophysiological Recordings. Recording sessions were exported from the TDT system to Plexon offline sorter using OpenBridge (Tucker-Davis Technologies, Alachua, FL, USA). Offline sorter (Plexon, Dallas, TX, USA) was used for sorting, and neural responses to cues and light stimulation were visualized through peristimulus time histograms (PSTH) and rasters for every unit using NeuroExplorer. Data from Plexon and Neuroexplorer data files was then imported into MATLAB and analyzed using Matlab software written by P.N. PSTHs were computed with 50 ms bins around onset

of CS and US presentation, and with 1 ms bins for responses evoked by light stimulation. Only trials with correct responses (at least one lick for sucrose trials, and no licks for quinine trials) were included in the PSTH. The CS PSTHs were z-transformed using the histogram values in a 2 s baseline period prior to the onset of the CS. The US PSTHs were z-transformed using the histogram values in a 2 s baseline period starting 3 s prior to the onset of the US. Similarly, PSTHs around a light pulse (used for photoidentification of BLA projectors) were z-transformed using a baseline window of 40 ms prior to the onset of the light pulse. To test significance of neural responses, Wilcoxon signed-rank test was performed on the neural activity of each unit by comparing the number of spikes in a baseline window (as described for z-transform) and an experimental window starting at the onset of CS or US. The US was presented between 300 ms and 1 s after the start of the CS, but the delay was constant within a session. For sessions where the CS-US interval was below 500 ms, the experimental window for CS response was chosen to be the CS-US interval, and for all other cases, it was set to 500 ms. The experimental window for US response was set to 500 ms. The experimental window for light response was set based on the results of the *ex vivo* experiment – 9 ms in animals with NAc projectors expressing ChR2 and 6 ms in all other animals. Significance threshold for the Wilcoxon signedrank test was set at $p < 0.01$.

Based on the outcome of the signed-rank tests to positive (sucrose-predictive) and negative (quinine-predictive) CS, and the sign of the z-score in the experimental window (indicating excitation/inhibition), each unit was classified into one of 9 mutually exclusive categories – (1) excited to positive CS only, (2) excited to negative CS only, (3) excited to both CS, (4) excited to positive CS and inhibited to negative CS, (5) inhibited to positive CS only, (6) inhibited to negative CS only, (7) inhibited to both CS, (8) inhibited to positive CS and excited to negative CS, and (9) non-responsive to both CS.

A unit was called photo-responsive if it satisfied 3 criteria – (1) significance of the signed-rank test relative to the onset of the light pulse was < 0.01, (2) the average z-score in the experimental window was above 0.5, and (3) latency of the response to the light pulse was less than the threshold set by ex vivo experiments (9 ms for BLA-NAc projectors, and 6 ms for BLA-CeA and BLA-vHPC projectors). Latency to the light pulse was defined as the first bin in the PSTH to cross 4 standard deviations relative to the 100 ms baseline window (Figure 5A).

The baseline firing rate of each unit was defined as the average number of spikes per second in the entire recording session (Figure 5C,D). The action potential duration was measured as the time from trough of the AP to peak of the AP (Figure 5D).

Principal components analysis (PCA). In order to extract information from the dynamics of cue-triggered neural responses for each projector population for CS-S and CS-Q, we used principal components analysis (PCA). The z-transformed PSTH of each neuron (50 ms bins) between -500 ms and 500 ms (= 20 dimensions per neuron per cue) relative to cue-onset was used for the PCA analysis. In order to bring the neural responses from both CS-S and CS-Q to a common space, the z-score time course relative to CS-S and CS-Q for each neuron was given as two separate observations to the PCA, meaning that the number of observations given to the PCA analysis was 2 x # of neurons. Therefore, given that we have 1626 neurons, there were 3252 observations, and 20 variables (or dimensions) per observation. The data was transformed using the pca function in MATLAB. Data along each of the first two principal components (PC1 and PC2) were averaged across observations to generate the vectors in Figure 6C. For example, given that there are 38 NAc projecting BLA neurons, 38 observations for CS-S, one for each NAc projector, were averaged to obtain the position of the BLA-NAc CS-S vector in a space defined by PC1 and PC2. Similarly, 38 observations for CS-Q, one for each NAc projector, were averaged to obtain the position of the CS-Q vector for NAc projectors in the space defined by PC1 and PC2.

Confocal microscopy

Confocal fluorescence images were acquired with an Olympus FV1000 confocal laser scanning microscope using a 20x/0.75NA objective for viral injections and recording electrode placement images were acquired using the FluoView software (Olympus, Center Valley, PA). The center of the viral injection was chosen as the brightest fluorescent point in AP, ML and DV axes. To image collaterals of BLA projectors, we used a 60x/1.42NA oil immersion objective for imaging axons in five downstream targets – prelimbic cortex (PL), infralimbic cortex (IL), NAc, CeA and vHPC. For the 14 structures imaged in each of the 10 brains (Figure 3 and S3), we matched all the imaging parameters (within each brain), including, laser intensity, photomultiplier tube voltage, gain and offset. The rest of the parameters remained constant for all images acquired – laser wavelength, pixel dwell time (2 µs/pixel), image XY resolution (0.207 µm/pixel), and imaging area (212 µm x 212 µm), Z-resolution (0.67 µm), confocal pinhole size (200 µm). Images were acquired across a total optical section thickness of 24 µm (36 slices).
Fluorescence was quantified using custom MATLAB software, written by PN. Digitized TIF images were imported into MATLAB, and fluorescence values were encoded as a number between 0 and 4095. The value of each pixel in each image was divided by 4095, to bring the fluorescence intensity range between 0 and 1. The images were then z-projected across 36 slices using a maximum intensity projection. A thresholding procedure was used to separate axon fluorescence from background. A threshold of 0.5 was set across all images in the green (ChR2-eYFP) channel, and a threshold of 0.8 was set across all images in the red (synaptophysin-mCherry) channel. These thresholds were chosen by an experimenter (blind to the imaged area and animal) observing the results of thresholding with different threshold values across multiple images (~ 15-20 images). Fluorescence was quantified as the fraction of pixels in the image above this threshold.

Statistical analysis

Statistical analyses were performed using Matlab or a commercial software (GraphPad Prism; GraphPad Software, Inc, La Jolla, CA). Changes in neural firing rate in response to the CS and US were tested using a Wilcoxon signed-rank test implemented in MATLAB with a significance threshold placed at $p<0.01$ (Figure 2B). Paired statistical comparisons of the *ex vivo* photoresponse latencies were made with a two-tailed paired Student t-test (Figure 4F). The distribution of *in vivo* photoresponse latency was done by comparing the projector populations to each other (3 comparisons) using a two-sample Kolmogorov-Smirnov test in Matlab and corrected for multiple comparisons (Figure 5B). The distribution of basal firing rate was compared between the BLA and the three projector populations (BLA to BLA-NAc, BLA to BLA-CeA and BLA to BLA-vHPC comparison) using a two-sample Kolmogorov-Smirnov test corrected for multiple comparisons (Figure 5C-D). Comparison of the z-scores differences was realized with a non-parametric Kruskal-Wallis test (Figure 6B). Finally, comparison of proportion of excitation and inhibition selectively to one cue (or one US delivery) were performed using a binomial test (Figure 7D). Threshold for significance was placed at $^{+}p<0.1$, $*p<0.05$, $**p<0.01$ and $***p<0.001$). All data are shown as mean ± standard error of the mean (SEM).